


 Cite this: *RSC Adv.*, 2024, 14, 36886

# Regulation of oxidative stress enzymes in *Candida auris* by Dermaseptin: potential implications for antifungal drug discovery

 Mohmmad Younus Wani, <sup>\*a</sup> Vartika Srivastava, <sup>bc</sup> Tamer S. Saleh, <sup>a</sup>  
 Abdullah Saad Al-Bogami, <sup>a</sup> Faisal Mohammed Aqlan<sup>a</sup> and Aijaz Ahmad <sup>\*bd</sup>

The emergence of *Candida auris* poses a significant global health threat due to its high mortality rates and multidrug resistance. The development of new antifungal drugs is essential to effectively combat this pathogen. Antimicrobial peptides, such as Dermaseptin, have demonstrated potent anti-*Candida* activity. This study aimed to investigate the antifungal activity of Dermaseptin against *C. auris* isolates and its ability to induce oxidative stress and apoptosis. The results revealed the robust anti-*Candida* activity of Dermaseptin, with a minimum inhibitory concentration (MIC) of 15.62  $\mu\text{g mL}^{-1}$  and a minimum fungicidal concentration (MFC) of 31.25  $\mu\text{g mL}^{-1}$ . Spectrophotometric analysis demonstrated that Dermaseptin induced significant oxidative stress, as evidenced by the notable differences in the activity of primary antioxidant enzymes and lipid peroxidation (LPO) levels between the treated and untreated control groups. Moreover, Dermaseptin influenced the gene expression of antioxidant enzymes, as confirmed by reverse transcription quantitative polymerase chain reaction (RT-qPCR). Additionally, Dermaseptin induced apoptosis in *C. auris* in a dose-dependent manner. This study highlights the potential of Dermaseptin to inhibit and potentially eradicate *C. auris* by increasing oxidative stress levels. The low MICs and fungicidal properties of Dermaseptin against *C. auris* isolates suggest its potential as a candidate for the development of a novel antifungal agent.

 Received 4th September 2024  
 Accepted 12th November 2024

DOI: 10.1039/d4ra06392a

[rsc.li/rsc-advances](http://rsc.li/rsc-advances)

## 1. Introduction

Microbial infections pose a significant global health challenge, with the emergence of multidrug-resistant pathogens exacerbating the problem. *Candida auris* is a relatively recent species of opportunistic fungi with distinct characteristics that contribute to its ability to colonize the skin and non-human surfaces.<sup>1</sup> This feature facilitates its rapid and efficient transmission between individuals. In addition to skin colonization, *C. auris* has been found to infect various sites in hospitalized patients and individuals with compromised immune systems, including the bloodstream, gastrointestinal tract, wounds, and ears. Globally reported cases of *C. auris* infection have been associated with significant outbreaks, and the mortality rate ranges from approximately 32% to 66%.<sup>2</sup> One of the major concerns regarding *C. auris* is its multidrug-resistant (MDR) nature, particularly in healthcare settings. This pathogen has

demonstrated resistance or reduced susceptibility to commonly used antifungal drugs, making it a significant nosocomial threat on a global scale.<sup>3–5</sup> While healthy individuals typically possess immune systems capable of recognizing and eliminating *C. auris*, immunocompromised patients are highly susceptible to fungal infections due to their weakened immune response.<sup>6</sup> Consequently, immunocompromised individuals are at a high risk of developing severe *C. auris* infections, as their immune systems are unable to effectively detect and combat invading fungi. Conventional antibiotics, once considered the cornerstone of infection management, are facing increasing limitations due to the rapid development of resistance mechanisms. In this context, the exploration of alternative therapeutic strategies becomes imperative.

Antimicrobial peptides (AMPs) have emerged as a promising avenue for combating microbial infections.<sup>7</sup> These small, naturally occurring defence molecules are found in various organisms, ranging from humans to microorganisms, and exhibit potent antimicrobial activity against a broad spectrum of pathogens, including bacteria, fungi, viruses, and parasites. Among the diverse repertoire of AMPs, Dermaseptin, a specific antimicrobial peptide, has garnered attention due to its intriguing properties and potential therapeutic applications.<sup>8</sup> The primary role of antimicrobial peptides, including Dermaseptin, lies in the innate immune system's defence against microbial invaders. AMPs serve as the first line of defence by

<sup>a</sup>Department of Chemistry, College of Science, University of Jeddah, 21589 Jeddah, Saudi Arabia. E-mail: mwani@uj.edu.sa

<sup>b</sup>Department of Clinical Microbiology and Infectious Diseases, School of Pathology, Faculty of Health Sciences, University of the Witwatersrand, South Africa. E-mail: aijaz.ahmad@wits.ac.za

<sup>c</sup>Department of Inflammation and Immunity, Lerner Research Institute, Cleveland Clinic, Cleveland, Ohio, 44195, USA

<sup>d</sup>Division of Pulmonary, Allergy, and Critical Care Medicine, Department of Medicine, University of Pittsburgh Medical Center, Pittsburgh, PA 15213, USA


targeting and neutralizing pathogens through multiple mechanisms.<sup>9,10</sup> One of the fundamental mechanisms involves the disruption of microbial cell membranes, where AMPs interact with lipid bilayers, forming pores or channels that compromise membrane integrity. This disruption leads to the leakage of intracellular components, ion imbalances, and subsequent cell death. Furthermore, some AMPs can penetrate microbial cells and directly interact with essential intracellular components, such as nucleic acids or proteins, disrupting their normal functions and inhibiting vital cellular processes.<sup>11</sup> Additionally, AMPs possess immunomodulatory properties, facilitating immune cell recruitment, promoting wound healing, and enhancing pathogen clearance.

In parallel, cells of the innate immune system serve as the primary line of defence against fungal infections. Upon encountering the fungus, an intracellular signalling cascade is triggered, leading to the generation of excessive reactive oxygen species (ROS) and inflicting irreversible cell damage, eventually resulting in cell death.<sup>12</sup> While aerobic organisms naturally produce ROS as by-products of cellular respiration, they employ a dynamic antioxidant defence mechanism to handle excess ROS, aiding the establishment of infection.<sup>13</sup> In *Candida albicans*, this defence mechanism is well-defined. The upregulation of the regulatory CAP1 gene orchestrates the synthesis of crucial antioxidant enzymes, including catalase (CAT), superoxide dismutase (SOD), glutathione peroxidase (GPx), reductase (GR), and transferase (GST).<sup>13</sup> These enzymes repair damages induced by oxidative stress, enabling fungal survival and persistence.

With this background, this investigation aims to assess the antifungal efficacy of Dermaseptin against *Candida auris*. Specifically, the study focuses on evaluating the impact of Dermaseptin on the enzymes involved in countering oxidative stress, along with analysing its effect on the gene expression of these antioxidant enzymes. Additionally, lipid peroxidation and cellular apoptosis, key processes associated with oxidative damage, will be evaluated. By scrutinizing these aspects, this research seeks to unravel the potential mechanisms underlying the antifungal activity of Dermaseptin against *C. auris*, particularly in relation to oxidative stress response pathways. Understanding the interplay between antimicrobial peptides, such as Dermaseptin, and the intricate antioxidant defence mechanisms of fungal pathogens will contribute to the development of novel therapeutic strategies.

## 2. Materials and methods

### 2.1. Yeast population

*C. auris* strains (MRL 4000, MRL 5762, MRL 5765, and MRL 6057), *C. albicans* SC5314, and *C. albicans* ATCC 90028 were stored in glycerol stocks at  $-80\text{ }^{\circ}\text{C}$ . Before starting the experiment, the culture was revived from glycerol stocks on Sabouraud Dextrose Agar (SDA) plates. A single colony was then cultured for 24 h in 10 mL of Sabouraud Dextrose Broth (SDB). Cell harvesting involved collecting cells, washing them with sterile distilled water, and counting using a hemocytometer. The cell concentration was then adjusted to  $10^7$  cells per mL in SDB supplemented with 1% glucose before use.

### 2.2. Antifungal susceptibility profiling

Antifungal susceptibility profiling was performed by broth microdilution assay as demonstrated by the European Committee on Antimicrobial Susceptibility Testing (EUCAST).<sup>14,15</sup> In summary, *Candida* cells ( $1.5 \times 10^5$  cells per mL or 0.5 Mcfarland) were resuspended in SDB supplemented with glucose (1%). An aliquot (100  $\mu\text{L}$ ) of the *C. auris* suspensions was inoculated in each dilution (100  $\mu\text{L}$ ) of Dermaseptin prepared at various concentrations (1000–0.48  $\mu\text{g mL}^{-1}$ ). Amphotericin B (AmB), with a concentration ranging from 0.25–128  $\mu\text{g mL}^{-1}$  and 0.031–16.0  $\mu\text{g mL}^{-1}$ , was used as a positive control for *C. auris* and *C. albicans*, respectively. Additionally, cells without any intervention were considered as a negative control. The plates were incubated for 24 h at  $37\text{ }^{\circ}\text{C}$ . The readings were taken on the xMark microplate spectrophotometer (Bio-Rad). The minimum inhibitory concentration (MIC) was established as the lowest concentration that completely hindered the growth of *C. auris*. The experiments were replicated independently three times, each in triplicate.

In a parallel setting, the minimum fungicidal concentration was determined as described previously.<sup>16</sup> Briefly, the MFC was determined by sub-culturing 10  $\mu\text{L}$  from wells exhibiting no turbidity onto SDA plates, followed by incubation at  $37\text{ }^{\circ}\text{C}$  for 24 hours. The MFC was identified as the lowest concentration without observable growth. All experiments were conducted in triplicate.

### 2.3. Effect on pre-formed biofilm using crystal violet assay and confocal microscopy

The *in vitro* anti-biofilm activity of the test compound on mature *C. auris* biofilm was evaluated. To perform this experiment, 100  $\mu\text{L}$  of cell suspension ( $1.0\text{--}5.0 \times 10^6$  cells per mL) was prepared in RPMI1640 media (pH 7.0) supplemented with 2% glucose and seeded in a flat bottom 96-well microplate and incubated at  $37\text{ }^{\circ}\text{C}$  for 24 h. After incubation, the unattached *C. auris* cells were gently aspirated and all the wells were washed at least thrice with the help of phosphate-buffered saline (PBS). The test compound (MIC, and  $2 \times \text{MIC}$ ) was then added to the defined wells of the microtiter plate and incubated for 24 h at  $37\text{ }^{\circ}\text{C}$ . After overnight incubation, the 96-well plates were again washed thrice with PBS and the wells were loaded with crystal violet (0.1%; 100  $\mu\text{L}$ ) and kept for 5 minutes at room temperature. Then the plates were given PBS washing thrice, followed by adding HCl-isopropanol (0.04 N; 150  $\mu\text{L}$ ) and sodium dodecyl sulfate (0.25%; 50  $\mu\text{L}$ ). The absorbance (590 nm) was recorded with the help of a microplate reader. The growth control was the untreated biofilm, and the values of the test samples and growth control were used to calculate the percentage of inhibition in mature biofilm.

$$\text{Biofilm inhibition rate} = \left( \frac{\text{OD control} - \text{OD sample}}{\text{OD control}} \right) \times 100$$

The crystal violet assay was further confirmed using confocal laser scanning microscopy (Srivastava and Ahmad, 2020a).<sup>5</sup> In



a parallel experiment, the compound-treated (MIC and 2× MIC) and untreated 24 h mature biofilm were stained with fluorescent dyes FUN-1 and ConA-Alexa Fluor 488 conjugate (45 minutes in dark). The slides were visualized using a confocal microscope CLSM-780 and Airyscan. The images were captured in a multitrack mode (FUN-1, Ex/Em = 543/560 nm; ConA, Ex/Em = 488/505 nm). The ConA dye can conjugate with the biofilm matrix and fluorescence green whereas FUN-1 stains the live cells and gives red fluorescence.

#### 2.4. Enzyme assays

Antioxidant enzymes released by *Candida* species are catalase (CAT), superoxide dismutase (SOD), glutathione peroxidase (GPx), glutathione reductase (GR) and glutathione *S*-transferase (GST). The protocol to study the effect of Dermaseptin in generating oxidative stress in *C. auris* was adopted from a previous work.<sup>17</sup> In summary, the *C. auris* cells propagated to their mid-log phase, washed with Phosphate Buffer Saline (PBS) and resuspended in sterile SDB with (test set) or without (control set) Dermaseptin (0.5 × MIC and MIC) and allowed to grow at 37 °C, 200 rpm for 4 hours. Later, the activity of CAT, SOD, GPx, GR and GST were quantified in both test as well as the control sets. Similarly, the extent of lipid peroxidation (LPO) in the absence and presence of Dermaseptin was expressed as nmol of TBARS (thiobarbituric acid-reactive substances) produced.

#### 2.5. RT-qPCR

The RT-qPCR methodology was adopted to study the effect of Dermaseptin on the expression of the various crucial antioxidant genes in *C. auris*. The yeast cells (0.5 Mcfarland) were exposed to Dermaseptin (MIC) for 4 hours at 37 °C. Total RNA extraction was performed using the Zymo Research Quick-RNA Fungal/Bacterial Miniprep Kit (Zymo Research Corp) and a Nanodrop spectrophotometer was used to assess the final concentration and purity of the obtained RNA. Subsequently, cDNA synthesis followed the manufacturer's instructions of the iScript™ cDNA Synthesis Kit (Bio-Rad).

Primers for antioxidant genes (*CATA*, *SOD4*, *GPx3*, *GST1*, and *GSHR*), along with a housekeeping gene (*ACT1*), were obtained from previous work.<sup>17</sup> An initial gradient PCR was carried out as described by the researcher to get an optimal annealing temperature (55 °C). Subsequently, RT-qPCR was carried out using the PowerUp™ SYBR™ Green Master Mix in a Bio-Rad CFX 96 qPCR System (USA). Thermal cycling conditions for RT-qPCR included UDG activation at 50 °C for 2 minutes, initial denaturation at 95 °C for 2 minutes, followed by 40 cycles of denaturation at 95 °C for 15 seconds, annealing at 55 °C for 30 seconds, and extension at 72 °C for 1 minute. The system automatically provided melt curve and  $C_q$  values, with dissociation curve conditions as follows: pre-melting at a ramp rate of 1.6 °C s<sup>-1</sup>, 95 °C for 15 seconds; melting at a ramp rate of 1.6 °C s<sup>-1</sup>, 60 °C for 1 minute; melting at a ramp rate of 0.15 °C s<sup>-1</sup>, 95 °C for 15 seconds. The analysis of gene expression was done concerning the housekeeping gene (*ACT1*) using the formula  $\Delta C_q = 2^{(C_{q \text{ target gene}} - C_{q \text{ reference gene}})}$ . The relative change in the expression was estimated by normalizing to housekeeping gene (*ACT1*) (Table 1).

Table 1 Nucleotide sequences for primers (5'–3')<sup>a</sup>

| Gene        | Primer sequences      |                      |
|-------------|-----------------------|----------------------|
|             | Forward (5'–3')       | Reverse (3'–5')      |
| <i>CATA</i> | GTGGATCGACTCTGGGTTGT  | CAAGAGGCTTCTCCACCAAG |
| <i>SOD4</i> | TCAACCCCTTACCACGGCTAC | CACCACCACAGACAAGTTGG |
| <i>GPX3</i> | CTACATCTCAACCGCAGCAA  | GCACTTTTCGCCTGAAGAAC |
| <i>GST1</i> | GGGGTCCCAATACCCTCT    | CTTGAACAAGGGCAGAGGAG |
| <i>GSHR</i> | CCATTGCCCAAAACACTCT   | CAACTTGGTCATTCTGGTGT |
| <i>ACT1</i> | ACGCACATCGACATCACATT  | CCTCTCAGTCGTCGGCTATC |

<sup>a</sup> *CATA*, peroxisomal catalase; *SOD4*, cell surface superoxide dismutase; *GPX3*, glutathione peroxidase-like peroxidoredoxin HYR1; *GST*, glutathione *S*-transferase 1; *GSHR*, glutathione reductase; *ACT1*, actin.

#### 2.6. Annexin V-FITC/PI staining assay

Annexin V-FITC/PI staining was performed to evaluate the apoptotic ability of Dermaseptin. The transfer of phosphatidylserine to the outer portion of the cell membrane denotes the onset of apoptosis and this phenomenon can be traced by using annexin V-FITC Apoptosis Detection Kit I (BD, USA).<sup>16</sup> Briefly, the cells were treated with different concentrations of Dermaseptin (0.5 × MIC and MIC), untreated negative control and H<sub>2</sub>O<sub>2</sub> (10 mM) treated positive control were used. The treated cells (0.5 Mcfarland) were mixed in 1× binding buffer and mixed with 5 μL each of Propidium Iodide (PI) and annexin V-FITC. Thereafter, samples were kept in a dark room for 15 min. Binding buffer (400 μL) was again added to each sample followed by analysis through a Flow cytometer (BD, USA) and FlowJo\_V10 software was used for analyzing the results. The obtained cell population was segregated into 4 quadrants (Q), Q1: necrosis (Annexin V<sup>-</sup>/PI<sup>+</sup>); Q2: late apoptosis (Annexin V<sup>+</sup>/PI<sup>+</sup>); Q3: early apoptosis (Annexin V<sup>+</sup>/PI<sup>-</sup>), Q4: viable cells (Annexin V<sup>-</sup>/PI<sup>-</sup>).

#### 2.7. Cytotoxicity studies

Dermaseptin was evaluated for its cytotoxic activity by using horse erythrocytes. The horse erythrocytes were obtained by centrifuging horse blood at 4000 rpm for 10 minutes. The collected erythrocytes were washed with PBS (cold) and resuspended in the same resulting in a 10% solution. The solution was again diluted with the help of cold PBS and the final working solution (1 : 10) was prepared. An aliquot (100 μL) of erythrocytes was subjected to Dermaseptin (0.5 × MIC, MIC and MFC) and incubated for 1 hour at room temperature. The erythrocytes were then centrifuged (4000 rpm for 10 minutes) and the supernatant was secured and analysed at 450 nm using a multi-mode microplate reader. The experiment included Triton X-100 (1%) and PBS were used as positive and negative controls, respectively. The degree of hemolysis was estimated by the formula.<sup>18</sup>

$$\% \text{ hemolysis} = \frac{[(A450 \text{ of treated sample}) - (A450 \text{ of negative control})]}{[(A450 \text{ of positive control}) - (A450 \text{ of negative control})]} \times 100$$



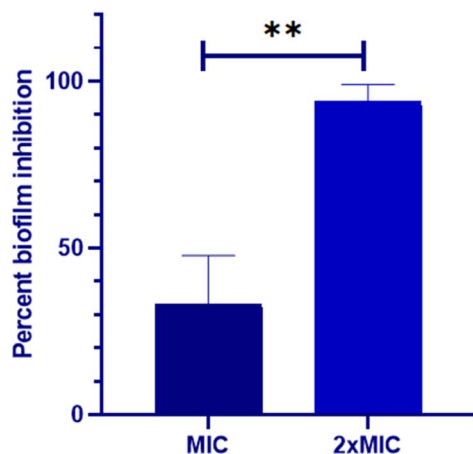


Fig. 1 Biofilm inhibition property of Dermaseptin against *C. auris*. Two dilutions (MIC and MFC) were used to examine the anti-biofilm effect of Dermaseptin. \*\* $P < 0.005$ .

## 2.8. Statistical analysis

Each experiment was conducted a minimum of three times, and the resulting values were presented as means  $\pm$  SD. Statistical analysis to assess the significance of differences between the control group (absence of Dermaseptin) and the test groups (presence of Dermaseptin) was performed through a one-way ANOVA. Significance was attributed to  $p$  values  $\leq 0.05$ . The data analysis was executed using GraphPad Prism software.

## 3. Results and discussion

### 3.1. Antifungal activity of Dermaseptin

Dermaseptin displayed strong antifungal activity against all tested strains of *Candida*, most notably against *C. auris* strains. The MIC and MFC values of Dermaseptin against *C. albicans* strains were recorded as  $0.125 \mu\text{g mL}^{-1}$  and  $0.25 \mu\text{g mL}^{-1}$ , respectively. Whereas the MIC and MFC values of Dermaseptin against *C. auris* strains ranged from  $7.81$ – $15.62 \mu\text{g mL}^{-1}$  and  $15.62$ – $31.25 \mu\text{g mL}^{-1}$ , respectively. Furthermore, in contrast to *C. albicans*, the *C. auris* strains displayed a high antimicrobial susceptibility profile against AmB; the MIC and MFC values of AmB against *C. auris* were  $4 \mu\text{g mL}^{-1}$  and  $8 \mu\text{g mL}^{-1}$ , respectively. The *C. auris* strain displaying the highest MIC and MFC values was selected for in-depth analysis. Researchers have demonstrated the antifungal activity of Dermaseptin against *C. albicans*,<sup>19–21</sup> furthermore, the obtained results are comparable to other tested antimicrobial peptides<sup>22</sup> and other Dermaseptins isolated from frog skin.<sup>23</sup>

### 3.2. Anti-biofilm activity of Dermaseptin

The impact of Dermaseptin on 24 hour mature biofilm was assessed using the crystal violet assay. Fig. 1 illustrates the percentage of biofilm inhibition at various concentrations tested. Treatment with MIC value led to an average reduction of mature biofilms by  $33.1\% \pm 14.66$  compared to the untreated control whereas, an average percent inhibition of  $93.76\% \pm 5.1$

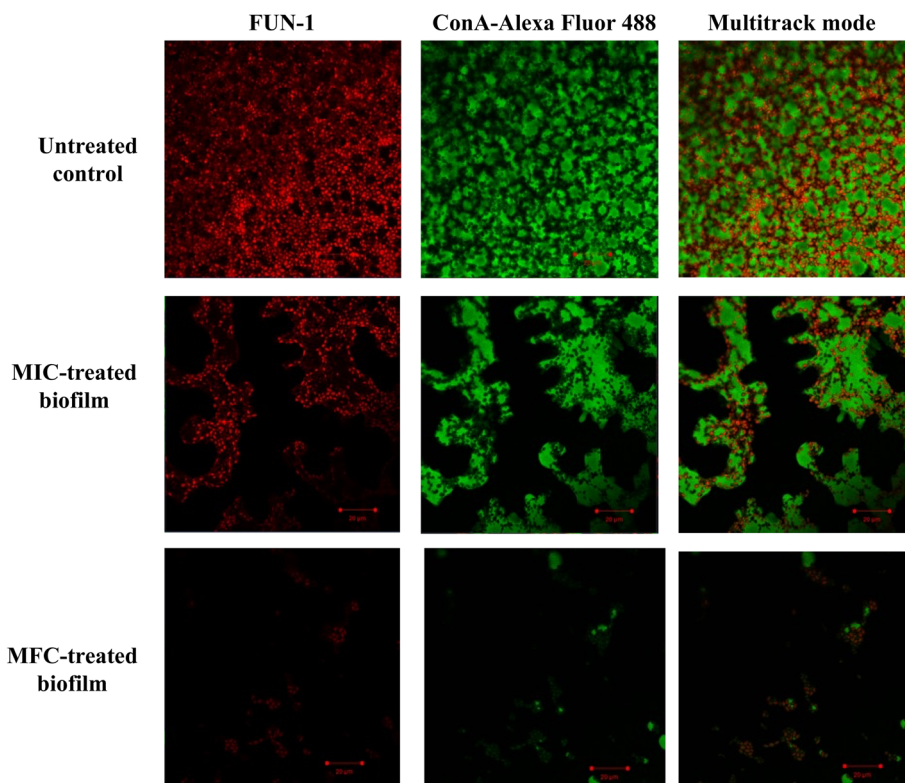


Fig. 2 Confocal microscopy of 24 h mature *C. auris* biofilm. In the micrographs, the green fluorescence, generated by ConA-Alexa Fluor 488, indicates the presence of the *C. auris* biofilm matrix. Conversely, the red fluorescence, emitted by FUN-1, signifies the presence of viable and metabolically active cells within the biofilm.



was observed at the MFC value. These findings suggest that the antibiofilm activity of Dermaseptin is concentration dependent. Moreover, confocal microscopy images, depicted in Fig. 2, corroborated the results of the crystal violet assay, confirming the anti-biofilm activity of Dermaseptin. In the untreated control sample, numerous metabolically active *C. auris* cells were observed, forming a well-defined and dense biofilm matrix exhibiting bright green fluorescence (from ConA-Alexa Fluor 488 conjugate dye), with embedded cells fluorescing red (from FUN-1 dye). Treatment with various doses of Dermaseptin (ranging from MIC to MFC) revealed its ability to disrupt the biofilm. At higher concentrations (MFC), the compound

effectively destroyed the mature biofilm, as evidenced by diminished green and red fluorescence compared to the untreated control. These results indicate the compound's capacity to penetrate the biofilm matrix, thereby impacting the viability of yeast cells embedded within and resulting in successful anti-biofilm activity.

### 3.3. The effect of Dermaseptin on antioxidant enzymes

The impact of Dermaseptin on the activity of crucial antioxidant enzymes in *C. auris* was evaluated (Fig. 3). Furthermore, the obtained data in LPO was correlated with the induction of oxidative stress in *C. auris*. The overall result demonstrated an

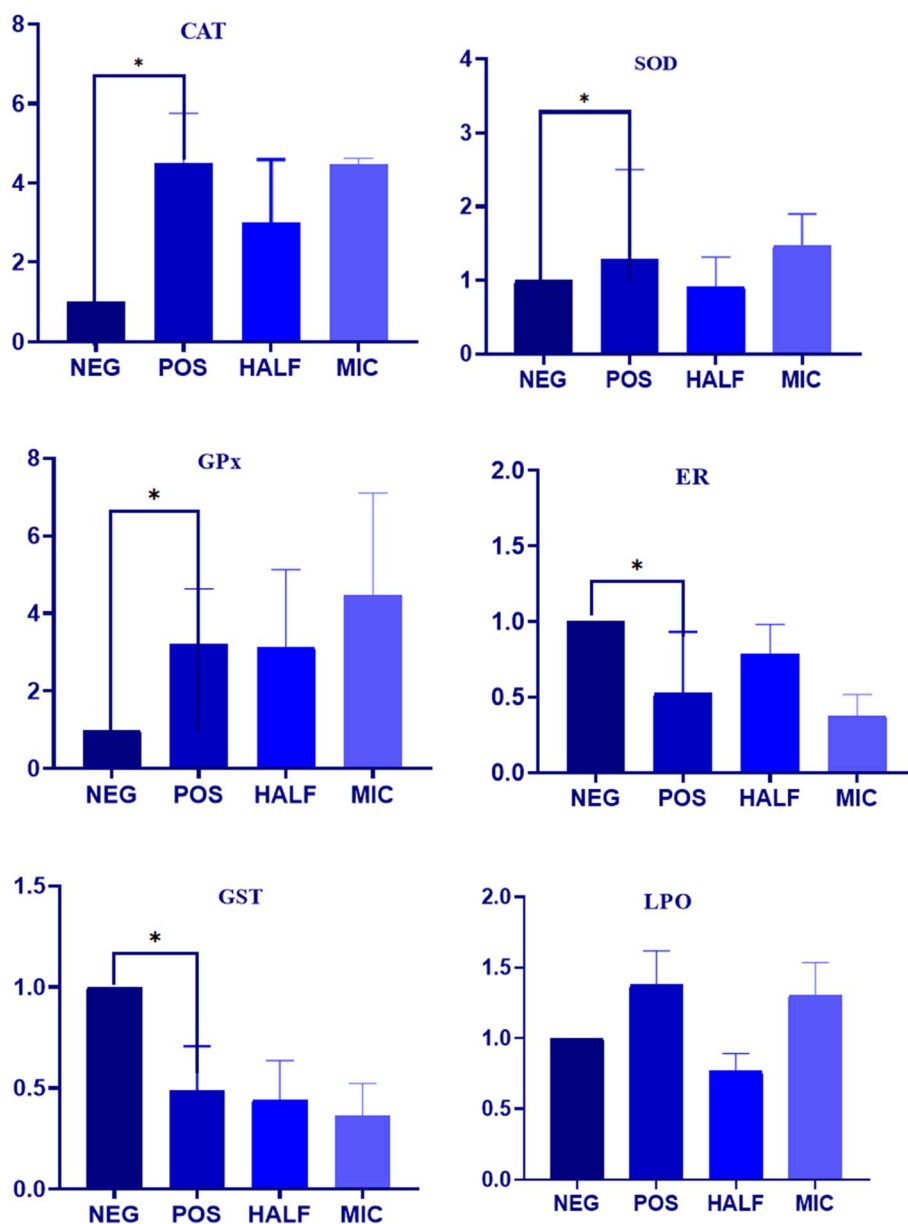


Fig. 3 Impact of Dermaseptin on antioxidant enzyme activities. *C. auris* was exposed to various concentrations of Dermaseptin (0.5  $\times$  MIC and MIC). Untreated cells were used as a negative control. An increase in enzyme activity is displayed by (A) catalase, (B) superoxide dismutase and (C) glutathione peroxidase. Whereas a decrease in enzyme activity is displayed by (D) glutathione reductase and (E) glutathione transferase. (F) Additionally, an overall increase in lipid peroxidation was observed after exposure to Dermaseptin.  $*P < 0.005$ .



increase in the activity of primary antioxidant enzymes (CAT, SOD and GPx) whereas a decrease in the activity of GR and GST was reported in the treated samples as compared to the untreated control. The average fold increase in the activity of CAT was 2.99 and 4.47 in the  $0.5 \times \text{MIC}$ - and MIC-treated *C. auris* strain respectively. Similarly, the average fold increase for SOD enzymes was 0.91 and 1.46 in the  $0.5 \times \text{MIC}$ - and MIC-treated *C. auris* strain respectively. Furthermore, the activity of GPx increased by 3.13 and 4.47 46 folds in the  $0.5 \times \text{MIC}$ - and MIC-treated yeast as compared to the untreated controls. An increased level of ROS within aerobic organisms induces the activity of SOD and CAT which play a crucial role in the defence against oxidative stress by degrading  $\text{H}_2\text{O}_2$  with GPx maintaining the  $\text{H}_2\text{O}_2$  content; the secondary antioxidant enzymes, GR and GST, continuously supply glutathione and nicotinamide adenine dinucleotide phosphate (NADPH) to the primary antioxidant enzymes. Furthermore, GR plays a crucial role in preserving the intracellular glutathione redox ratio (GSH/GSSG), while glutathione S-transferase (GST) serves as a vital antioxidant enzyme, facilitating the detoxification of foreign agents.<sup>12,24</sup> The average decrease in the activity of GR was 0.78 and 0.37, and of GST was 0.44 and 0.36 in the  $0.5 \times \text{MIC}$ - and MIC-treated strain respectively as compared to the untreated control. In the current study, a decline in the activity of these enzymes was noted as *Candida* cells were subjected to escalating concentrations of Dermaseptin. These observations follow previous findings where researchers have explored the antifungal activity of compounds based on these enzymes in other *Candida* species.<sup>17,25,26</sup>

Notably, lipid peroxidation is considered a marker of oxidative stress produced by reactive oxygen species (ROS), and TBARS is an indicator to quantify LPO. The present results displayed a gradual increase in the rate of TBARS formation when cells were treated with increasing concentrations of Dermaseptin (Fig. 3). An increase in ROS levels within an organism leads to oxidative stress, often induced by external factors such as antifungal drugs, which render the cell membrane permeable and trigger cellular events such as DNA disorganization, lipid oxidation, and consequential structural and molecular modifications.<sup>27</sup> LPO stands out as a predominant manifestation of oxidative stress caused by ROS as it results in the disruption of the cellular structure and overall membrane functionality. This damage to lipids is reflected in the accumulation of TBARS in the cytoplasm.<sup>17</sup> The TBARS assay utilizes spectrophotometry to measure the reaction between malondialdehyde (MDA) and thiobarbituric acid (TBA) under strong acidic conditions and heating.<sup>28</sup> This investigation demonstrates that exposure to Dermaseptin induces the generation of LPO in *C. auris*, suggesting membrane disintegration. These findings align with prior studies on antifungal activity, particularly those examining LPO in other *Candida* strains.<sup>17</sup>

#### 3.4. Effect of Dermaseptin on gene expression

The transcriptional profile of genes encoding crucial oxidative stress enzymes (*CATA*, *SOD4*, *GPx3*, *GST1*, and *GSHR*) was assessed using RT-qPCR. Data analysis involved comparing

replicates of Dermaseptin-treated and untreated samples. A significant level of upregulation was observed in the genes encoding for the primary enzymes whereas, the genes encoding secondary enzymes displayed downregulation. Notably, *SOD4* demonstrated the highest level of expression with an average fold increase of 2.72, whereas *GSHR* showed the lowest expression with a fold change of 0.47. A summary of the differences in fold change is presented in Fig. 4.

To further substantiate the impact of Dermaseptin on the antioxidant enzymes of *C. auris*, the genetic expression levels of genes encoding these enzymes were investigated. Following treatment with Dermaseptin at the MIC value, the antioxidant genes (*CATA*, *SOD4*, *GPx3*, *GST1*, and *GSHR*) underwent RT-qPCR, with *ACT1* serving as a reference/housekeeping gene. Among the examined genes, *CATA*, *SOD4*, and *GPx3* exhibited a significant increase in expression. In contrast, *GST1* and *GSHR* were notably downregulated. The upregulation of *CATA* and *SOD4* genes post-Dermaseptin treatment confirms the induction of oxidative stress.

#### 3.5. Apoptotic activity of Dermaseptin

The onset of apoptosis exposes membrane protein (phosphatidylserine) to the outer side of the plasma membrane.<sup>29</sup> Thus, we included this experiment to validate the apoptotic property of Dermaseptin. The exposure of phosphatidylserine was determined with the help of the Annexin V + PI dual staining assay. During the process, Annexin V stains the exposed phosphatidylserine while PI validates plasma membrane integrity. Hence, this technique can discriminate between apoptotic, late apoptotic and necrotic cells (Fig. 5). In the untreated control, the majority of cells (90.4%) were confined to Q4 representing the presence of live cells in the sample. Whereas, treatment with Dermaseptin at  $0.5 \times \text{MIC}$  resulted in the migration of cells from Q4 (77.7%) to Q3 (21.5%), Q2 (2.6%) and Q1 (1.19%), representing the onset of early apoptosis; at a higher concentration of Dermaseptin (MIC), the maximum cellular population was found sitting in Q2 (91.5%) followed by Q1 (6.1%),

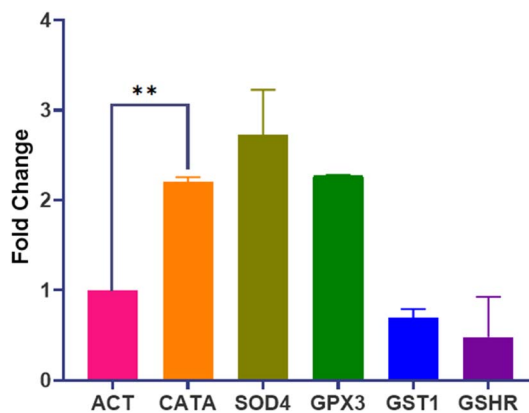


Fig. 4 Gene expression analysis in *C. auris*. Observed fold change in the genes encoding for the primary (*CATA*, *SOD4* and *GPx3*) and secondary (*GST1* and *GSHR*) antioxidant enzymes in response to Dermaseptin treatment.  $***P < 0.005$ .

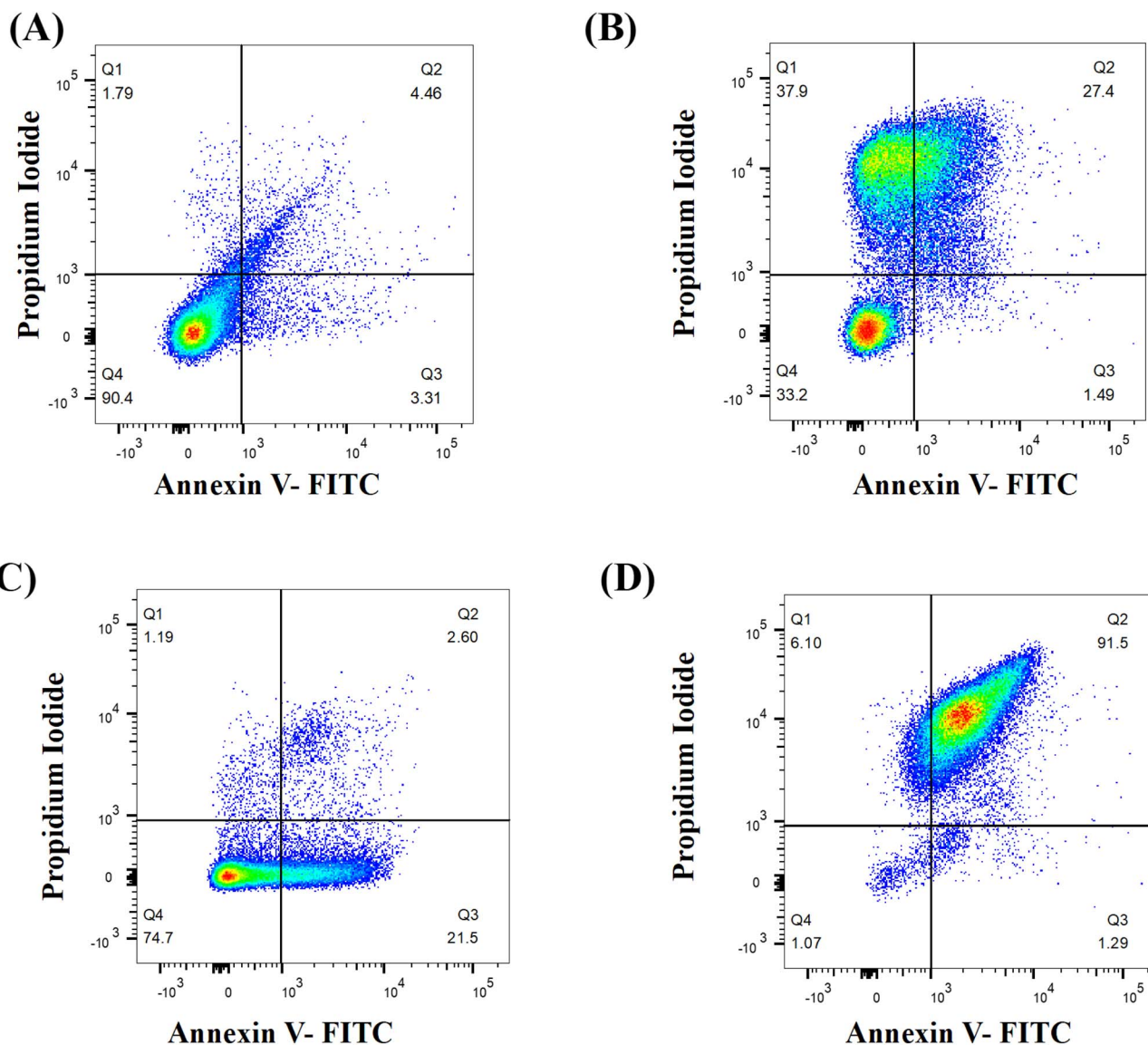


Fig. 5 Determination of the apoptotic activity of Dermaseptin by Annexin V-FITC + PI double staining technique. (A) Untreated control cells, (B) H<sub>2</sub>O<sub>2</sub> (10 mM) treated positive control and *C. auris* treated with 0.5 × MIC (C) and MIC (D) values of the test compound. Q1 represents necrosis (Annexin V<sup>-</sup>/PI<sup>+</sup>), Q2 represents late apoptosis (Annexin V<sup>+</sup>/PI<sup>+</sup>), Q3 represents early apoptosis (Annexin V<sup>+</sup>/PI<sup>-</sup>) and Q4 represents viable cells (Annexin V<sup>-</sup>/PI<sup>-</sup>).

Q3 (1.29%) and Q4 (1.07%) showing onset of late apoptosis. The data suggested that Dermaseptin has exerted dose-dependent cellular apoptosis in *C. auris*. Similarly, the cellular population in the positive control was dispersed in all the quadrants (37.9%, Q1; 27.4%, Q2; 1.49%, Q3 and 33.2%, Q4) suggesting exposure to H<sub>2</sub>O<sub>2</sub> triggered necrosis in *C. auris*.

### 3.6. Hemolysis activity of Dermaseptin

Based on the findings above, it is clear that Dermaseptin exhibits potent antifungal properties and influences the expression of antioxidant enzymes in *C. auris*. Consequently, it was essential to assess the cytotoxic effects of Dermaseptin. The results indicated that the percentage of hemolysis caused by Dermaseptin in horse erythrocytes ranges from 9.24% to 44.04% at a concentration of 0.5 × MIC to MFC (Fig. 6). At MIC value the average percentage of

hemolysis was 20.15%. Studies have previously reported that at higher concentrations, antimicrobial peptides tend to exhibit high toxicity at the haematological level and in different human

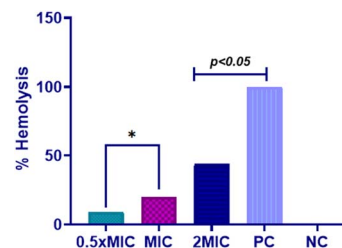


Fig. 6 Hemolysis assay. Hemolytic activity of Dermaseptin at varying concentrations. Positive control, 1% Triton X and negative control, PBS. PC: positive control, NC: negative control.



cell types.<sup>22,30</sup> It is worth mentioning that certain studies have suggested that modifying these antimicrobial peptides (AMPs) can mitigate their adverse impact, as observed in several amphibian-derived AMPs.<sup>30,31</sup>

## 4. Conclusion

The outcomes of this investigation strongly support the potential of Dermaseptin as an antifungal candidate, given its ability to impede the growth of multidrug-resistant *C. auris*. Furthermore, Dermaseptin has demonstrated the induction of oxidative stress, evident through the upregulation of LPO and the activity and gene expression of key antioxidant enzymes. These findings provide valuable insights for future experiments aimed at refining prescriptions and determining optimal concentrations of Dermaseptin in clinical settings for the prevention, management, and treatment of candidiasis.

While this study highlights the promising antifungal activity of Dermaseptin against *Candida auris*, further investigations are warranted to assess its stability in the presence of proteases, such as matrix metalloproteases, to better understand its potential therapeutic applications. Additionally, the possibility that Dermaseptin may elicit inflammatory responses *via* ROS generation in the human immune system remains to be explored. Future studies should focus on evaluating the interaction of Dermaseptin with immune cells, particularly macrophages, to assess any potential immunomodulatory effects. These investigations will be crucial for determining the overall safety profile of Dermaseptin as an antifungal agent.

## Data availability

All the data supporting this article have been included in the research article. If the raw data is required, it will be made available on request.

## Author contributions

(MYW): conceptualization, methodology, project administration, writing – original draft, writing – review & editing, funding acquisition, supervision. (VS): investigation, writing – review & editing. (TSS): methodology, formal analysis. (ASAL-B): methodology, formal analysis. (FMA): methodology, formal analysis. (AA): conceptualization, methodology, investigation, formal analysis, writing – original draft, writing – review & editing, visualization, supervision.

## Conflicts of interest

The authors declare that they have no known competing financial interests or personal relationships that could have appeared to influence the work reported in this paper.

## Acknowledgements

This work was funded by the University of Jeddah, Jeddah, Saudi Arabia, under grant no. (UJ-23-DR-264). Therefore, the

authors thank the University of Jeddah for its technical and financial support.

## References

- 1 S. K. Mishra, Y. Muhammad and W. Mark, *Candida auris*: an emerging antimicrobial-resistant organism with the highest level of concern, *Lancet Microbe*, 2023, **4**(7), e482–e483.
- 2 L. Rossato and A. L. Colombo, *Candida auris*: What Have We Learned About Its Mechanisms of Pathogenicity?, *Front. Microbiol.*, 2018, **9**(3081), 1–6, DOI: [10.3389/fmicb.2018.03081](https://doi.org/10.3389/fmicb.2018.03081).
- 3 S. Kathuria, P. K. Singh, C. Sharma, A. Prakash, A. Masih, A. Kumar, *et al.*, Multidrug-resistant *Candida auris* misidentified as *Candida haemulonii*: characterization by matrix-assisted laser desorption ionization–time of flight mass spectrometry and DNA sequencing and its antifungal susceptibility profile variability by Vitek 2, CLSI broth microdilution, and Etest method, *J. Clin. Microbiol.*, 2015, **53**(6), 1823–1830.
- 4 A. Chakrabarti, P. Sood, S. M. Rudramurthy, S. Chen, H. Kaur, M. Capoor, *et al.*, Incidence, characteristics and outcome of ICU-acquired candidemia in India, *Intensive Care Med.*, 2015, **41**, 285–295.
- 5 V. Srivastava and A. Ahmad, Abrogation of pathogenic attributes in drug-resistant *Candida auris* strains by farnesol, *PLoS One*, 2020, **15**(5), e0233102, DOI: [10.1371/journal.pone.0233102](https://doi.org/10.1371/journal.pone.0233102).
- 6 S. Latocha, *Candida auris*: A Quietly Emerging Health Threat, RGA ReFlections, 2020, available at: <https://www.rgare.com/knowledge-center/media/articles/Candida-auris-a-quietly-emerging-health-threat>, accessed November 2020.
- 7 Q. Y. Zhang, Z. B. Yan, Y. M. Meng, X. Y. Hong, G. Shao, J. J. Ma, X. R. Cheng, J. Liu, J. Kang and C. Y. Fu, Antimicrobial peptides: mechanism of action, activity and clinical potential, *Mil. Med. Res.*, 2021, **8**(1), 48, DOI: [10.1186/s40779-021-00343-2](https://doi.org/10.1186/s40779-021-00343-2).
- 8 E. J. H. Bartels, D. Dekker and M. Amiche, Dermaseptins, Multifunctional Antimicrobial Peptides: A Review of Their Pharmacology, Effectivity, Mechanism of Action, and Possible Future Directions, *Front. Pharmacol.*, 2019, **10**, 1421, DOI: [10.3389/fphar.2019.01421](https://doi.org/10.3389/fphar.2019.01421).
- 9 Y. Huan, Q. Kong, H. Mou and H. Yi, Antimicrobial Peptides: Classification, Design, Application and Research Progress in Multiple Fields, *Front. Microbiol.*, 2020, **11**, 582779, DOI: [10.3389/fmicb.2020.582779](https://doi.org/10.3389/fmicb.2020.582779).
- 10 D. I. Duarte-Mata and M. C. Salinas-Carmona, Antimicrobial peptides' immune modulation role in intracellular bacterial infection, *Front. Immunol.*, 2023, **14**, 1119574, DOI: [10.3389/fimmu.2023.1119574](https://doi.org/10.3389/fimmu.2023.1119574).
- 11 K. R. Gagandeep, B. N. Ramesh and V. V. Gatta, Unveiling mechanisms of antimicrobial peptide: actions beyond the membranes disruption, *Heliyon*, 2024, **10**(19), e38079, DOI: [10.1016/j.heliyon.2024.e38079](https://doi.org/10.1016/j.heliyon.2024.e38079).
- 12 D. Kaloriti, M. Jacobsen, Z. Yin, M. Patterson, A. Tillmann, D. A. Smith, *et al.*, Mechanisms underlying the exquisite sensitivity of *Candida albicans* to combinatorial cationic



- and oxidative stress that enhances the potent fungicidal activity of phagocytes, *MBio*, 2014, 5(4), 10–128.
- 13 S. Wang, G. He, M. Chen, T. Zuo, W. Xu and X. Liu, The role of antioxidant enzymes in the ovaries, *Oxid. Med. Cell. Longevity*, 2017, 2017, 4371714, DOI: [10.1155/2017/4371714](https://doi.org/10.1155/2017/4371714).
  - 14 J. L. Rodriguez-Tudela, M. C. Arendrup, F. Barchiesi, J. Bille, E. Chryssanthou, M. Cuenca-Estrella, *et al.*, EUCAST definitive document EDef 7.1: method for the determination of broth dilution MICs of antifungal agents for fermentative yeasts, *Clin. Microbiol. Infect.*, 2008, 14(4), 398–405, DOI: [10.1111/j.1469-0691.2007.01935.x](https://doi.org/10.1111/j.1469-0691.2007.01935.x).
  - 15 M. C. Arendrup, M. Cuenca-Estrella, C. Lass-Flörl and W. Hope, EUCAST-AFST. EUCAST technical note on the EUCAST definitive document EDef 7.2: method for the determination of broth dilution minimum inhibitory concentrations of antifungal agents for yeasts EDef 7.2 (EUCAST-AFST), *Clin. Microbiol. Infect.*, 2012, 18(7), E246–E247, DOI: [10.1111/j.1469-0691.2012.03880.x](https://doi.org/10.1111/j.1469-0691.2012.03880.x).
  - 16 V. Srivastava, M. Y. Wani, A. S. Al-Bogami and A. Ahmad, Piperidine based 1,2,3-triazolylacetamide derivatives induce cell cycle arrest and apoptotic cell death in *Candida auris*, *J. Adv. Res.*, 2020, 29, 121–135, DOI: [10.1016/j.jare.2020.11.002](https://doi.org/10.1016/j.jare.2020.11.002).
  - 17 M. Ismail, V. Srivastava, M. Marimani and A. Ahmad, Carvacrol modulates the expression and activity of antioxidant enzymes in *Candida auris*, *Res. Microbiol.*, 2022, 173(3), 103916, DOI: [10.1016/j.resmic.2021.103916](https://doi.org/10.1016/j.resmic.2021.103916).
  - 18 M. Y. Wani, S. S. M. Alghamidi, V. Srivastava, A. Ahmad, F. M. Aqlan and A. S. Al-Bogami, Click synthesis of pyrrolidine-based 1,2,3-triazole derivatives as antifungal agents causing cell cycle arrest and apoptosis in *Candida auris*, *Bioorg. Chem.*, 2023, 136, 106562, DOI: [10.1016/j.bioorg.2023.106562](https://doi.org/10.1016/j.bioorg.2023.106562).
  - 19 D. Savoia, R. Guerrini, E. Marzola and S. Salvadori, Synthesis and antimicrobial activity of dermaseptin S1 analogues, *Bioorg. Med. Chem.*, 2008, 16(17), 8205–8209.
  - 20 D. Shi, X. Hou, L. Wang, Y. Gao, D. Wu, X. Xi, *et al.*, Two novel dermaseptin-like antimicrobial peptides with anticancer activities from the skin secretion of *Pachymedusa dactylospora*, *Toxins*, 2016, 8(5), 144.
  - 21 A. Belmadani, A. Semlali and M. Rouabhia, Dermaseptin-S1 decreases *Candida albicans* growth, biofilm formation and the expression of hyphal wall protein 1 and aspartic protease genes, *J. Appl. Microbiol.*, 2018, 125(1), 72–83.
  - 22 K. Y. Lum, S. T. Tay, C. F. Le, V. S. Lee, N. H. Sabri, R. D. Velayuthan, *et al.*, Activity of novel synthetic peptides against *Candida albicans*, *Sci. Rep.*, 2015, 5(1), 9657.
  - 23 M. Harris, H. M. Mora-Montes, N. A. R. Gow and P. J. Coote, Loss of mannosylphosphate from *Candida albicans* cell wall proteins results in enhanced resistance to the inhibitory effect of a cationic antimicrobial peptide *via* reduced peptide binding to the cell surface, *Microbiology*, 2009, 155(4), 1058–1070, DOI: [10.1099/mic.0.026120-0](https://doi.org/10.1099/mic.0.026120-0).
  - 24 R. L. Peterson, A. Galaleldeen, J. Villarreal, A. B. Taylor, D. E. Cabelli, P. J. Hart, *et al.*, The phylogeny and active site design of eukaryotic Cu-only superoxide dismutases, *J. Biol. Chem.*, 2016, 40(291), 20911–20923, DOI: [10.1074/jbc.M116.748251](https://doi.org/10.1074/jbc.M116.748251).
  - 25 A. Marchese, C. R. Arciola, E. Coppo, R. Barbieri, D. Barreca, S. Chebaibi, *et al.*, The natural plant compound carvacrol as an antimicrobial and anti-biofilm agent: mechanisms, synergies and bio-inspired anti-infective materials, *Biofouling*, 2018, 6(34), 630–656, DOI: [10.1080/08927014.2018.1480756](https://doi.org/10.1080/08927014.2018.1480756).
  - 26 L. Sun, K. Liao, C. Hang and D. Wang, Honokiol induces reactive oxygen species-mediated apoptosis in *Candida albicans* through mitochondrial dysfunction, *PLoS One*, 2017, 2(12), 1–17, DOI: [10.1371/journal.pone.0172228](https://doi.org/10.1371/journal.pone.0172228).
  - 27 A. D. S. Dantas, A. Day, M. Ikeh, I. Kos, B. Achan and J. Quinn, Oxidative stress responses in the human fungal pathogen, *Candida albicans*, *Biomolecules*, 2015, 5(1), 142–165, DOI: [10.3390/biom5010142](https://doi.org/10.3390/biom5010142).
  - 28 E. Niki, Biomarkers of lipid peroxidation in clinical material, *Biochim. Biophys. Acta*, 2014, 1840, 809–817, DOI: [10.1016/j.bbagen.2013.03.020](https://doi.org/10.1016/j.bbagen.2013.03.020).
  - 29 C. Jia, J. Zhang, L. Yu, C. Wang, Y. Yang, X. Rong, *et al.*, Antifungal activity of coumarin against *Candida albicans* is related to apoptosis, *Front. Cell. Infect. Microbiol.*, 2019, 8, 445, DOI: [10.3389/fcimb.2018.00445](https://doi.org/10.3389/fcimb.2018.00445).
  - 30 X. Zhou, D. Shi, R. Zhong, Z. Ye, C. Ma, M. Zhou, *et al.*, Bioevaluation of Ranatuerin-2Pb from the Frog Skin Secretion of *Rana pipiens* and Its Truncated Analogues, *Biomolecules*, 2019, 9(6), 249, DOI: [10.3390/biom9060249](https://doi.org/10.3390/biom9060249).
  - 31 J. M. Conlon, S. Galadari, H. Raza and E. Condamine, Design of potent, non-toxic antimicrobial agents based upon the naturally occurring frog skin peptides, ascaphin-8 and peptide XT-7, *Chem. Biol. Drug Des.*, 2008, 72(1), 58–64.

